DERIVATION OF GLACIER VELOCITY FROM SAR AND OPTICAL DATA WITH FEATURE TRACKING

Lei Huang[1,2] *Zhen Li*[1]

[1]Center for Earth Observation & Digital Earth, Chinese Academy of Sciences, China
[2]Graduate University of Chinese Academy of Sciences, China

ABSTRACT

Monitoring temperate glacier activity has become more and more necessary for economical and security reasons and as an indicator of the local effects of global climate. The most studied variable in ice dynamics in the literature is ice velocity. From remotely sensed images, mainly two types of methods have been used for the estimation of glacier flow velocities: feature tracking and differential intererometry (DInSAR). In this paper velocities of the Keqikaer glacier are acquired from ALOS (Advanced Land Observing Satellite) optical and SAR data respectively with feature tracking. We show that different window size in correlation calculation of feature tracking leads to different flow field. We also developed a new method to determine the best window size, and the method is testified by the two kinds of data.

Keywords: Glacier velocity, featuring tracking, window size, cross correlation, ALOS

1. INTRODUCTION

Glaciers and ice caps provide among the most visible indications of the effects of climate change [1]. Recent evidence suggests an acceleration of glacier mass loss in many areas all over the world [2]. Monitoring temperate glacier activity has become more and more necessary for economical and security reasons and as an indicator of the local effects of global climate [3]. However, the temporal sparsity of velocity data has made it difficult to explain the nature of the relationships between thinning, acceleration and retreat in these glaciers.

Because of the difficulty of reaching high-altitude glaciers in risky mountainous areas, up to now, only 1% of the existing world temperate glacier have been monitored, mostly by ground measurements, which often provide information only once or twice a year at a few points [3]. Remote sensing provides new choices in the measurement of surface motion of glaciers. Radar interferometry and feature tracking are two methods usually used in former research, however, the successful use of differential SAR interferometry is limited by phase noise, usually characterized by the coherence. Optical and SAR image are both available for feature tracking, which are used together to make a comparison in this paper.

2 STUDY AREA AND DATA

Keqicar Baxi Glacier lying in Chinese west Tienshan Mountain is picked out as study area. It is a large dendritic mountain valley glacier. One of the distinct characteristics of Keqikaer glacier is the presence of debris covering a large portion of the ablation zone. Altitude above 3800 m a.s.l of the glacier is covered by snow and ice, altitude between 3020 and 3800 m a.s.l is covered by debris.

The data used in this paper are all from ALOS. The

PRISM (Panchromatic Remote-sensing Instrument for Stereo Mapping) data and PALSAR (Phased Array L-band SAR) data are employed. All available images for this study are listed in table 1.

Table 1. ALOS image used in the experiment

Date	Sensor	Path	Frame	A/D*
06/01/2007	PALSAR	514	820	A
24/02/2008	PALSAR	514	820	A
09/05/2007	PRISM	183	2760	D
09/06/2008	PRISM	182	2760	D

*A/D means Ascending or Descending

3. METHOD

3.1 Basic processes

Feature tracking in SAR imagery is similar to optical imagery, two coregistered satellite images of different times are employed. The method can be divided into three steps. Firstly, two images are accurately coregistered respectively. Secondly, cross correlation coefficient is calculated between two image patches. The first image (called master image) is divided into grid and each small window P search for its most similar counterpart window P' in the second image (called slavery image), as figure 1. The correlation coefficients determine similarity; coordinate displacement of the window and time interval determine flow velocity. The third step, 3D velocity correction. The velocity calculated from step 2 is a plane velocity from images, and the real velocity which is related to topography can be obtained with DEM data. More details can be found in [4].

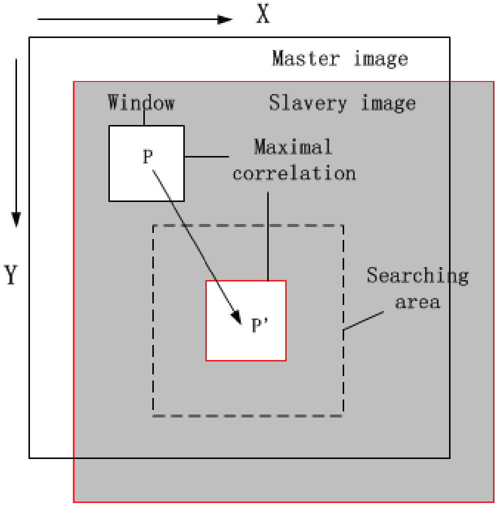

Figure 1. Sketch map of feature tracking

3.2 Window size

The window size is a significant parameter in calculating offset of images. In our experiment we will show the differences of flow fields acquired from different window size (figure 2) and illustrate how to get best window size.

The experiments are based on the hypothesis that velocities of a glacier change gradually on a large scale. According to mass balance, it is unreasonable if an individual window has much higher or lower velocity than its adjacent ones around. Windows with abnormal velocity that differ distinctively from around ones are considered as noises. AVG, which is defined as averaged velocity gradient, is introduced as equation (1):

$$AVG = \frac{\sum_{i=1}^{N} \sqrt{\left(\frac{Ry^2}{Rx^2 + Ry^2} \left(V_i(x,y) - V_i(x+n,y)\right)^2 + \frac{Rx^2}{Rx^2 + Ry^2} \left(V_i(x,y) - V_i(x,y+n)\right)^2 \right)}}{N} \tag{1}$$

Rx, Ry are window spacing in X and Y directions. $\frac{Rx^2}{Rx^2 + Ry^2}$ and $\frac{Ry^2}{Rx^2 + Ry^2}$ are weights assigned to different directions. In the equation n is the length of a window (n×n pixels contained in a window), $V_i(x,y)$ is velocity of the window in the coordinates of (x,y), while $V_i(x+n,y), V_i(x,y+n)$ are velocities of its adjacent windows. N is the total number of windows involved in calculation. Averaged velocity gradient expresses velocity variation of the whole flow field, and high AVG values denote intense changes.

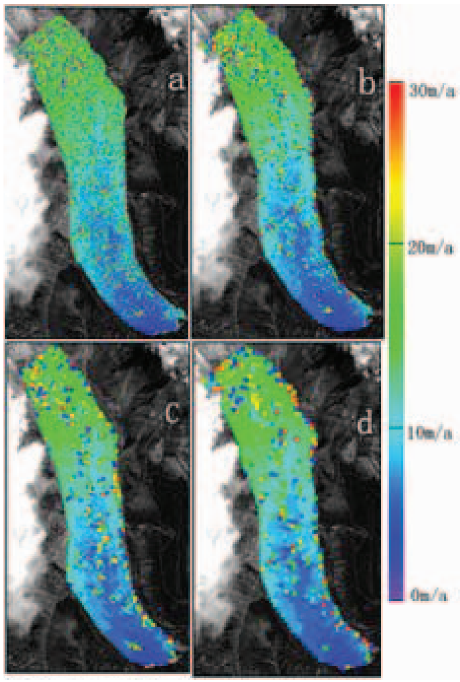

Figure 2. Glacier velocity resulted from different window sizes of optical images. a 10×10, b 20×20, c 30×30, d 40×40

Figure 2 reveals that optical images different window size leads to different velocity field, and averaged velocity gradient and noises decrease while window size increases. SAR images get the same conclusion, but they are not shown here because of space limitation. Relations between window size and AVG of the employed optical and SAR data are shown in figure 3.

In figure 3 AVG value changes abruptly while window size is small and the change becomes gentle while window size increases to a certain extent. While window size is small, noises from mismatches play the key role in rising AVG value, and the influence of noises shrinks as window size grow bigger and bigger. While AVG changes gently with window size we believe that noises are not the dominating factor of AVG changes anymore although they still exist. On the other side, as window size increases, center-to-center spacing between windows increases as well, losing velocity details and decreasing plane resolution of flow field. Considering the two sides, we pick the window size on the turning point that AVG curves shifts from abrupt to gentle as the optimal choice. In figure 6(*a*) we fit straight lines with every three continuous points in the curve from beginning to end. While the slope rate (slope rate $=\Delta AVG/\Delta G$, ΔAVG and ΔG are intercepts on the axes) of the fitted line becomes lower than 0.2, it is regarded as gentle slope, and the middle one of the three points is defined as turning point which corresponds with the best-size. With this method in the experiment, optical image gets its optimal size in 30×30 pixels while SAR image gets its optimal size in 50×50 pixels. In fact, flow field acquired from best window size is a tradeoff between velocity smoothness and velocity details.

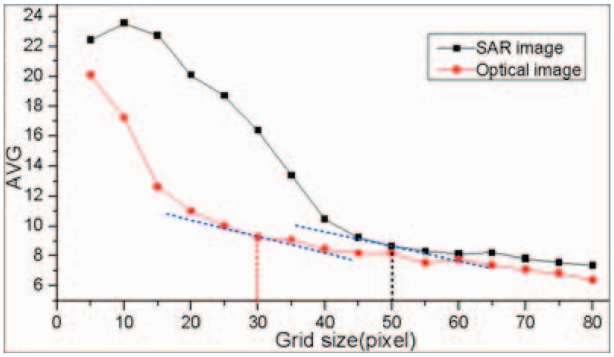

Figure 3. Curve of window size and AVG for optical and SAR images

3.3 Noise filter

Besides moving, other variations also exist on glaciers, such as melting, rocks rolling. Mismatches resulted from these variations are inevitable. According to our hypothesis in section 3.2, it is unreasonable if one single window get much different velocity from its adjacent ones, and it will be filtered out as noise. Ultimately, the gaps of the noise will be filled by linear interpolation. Being covered by snow and ice on the upper side of glacier, debris features on optical images is visible only below 3600 m a.s.l. Altitude above 4000 m a.s.l is so steep that the glacier is overlaid and shadowed by mountains in SAR image. Flow field from SAR and optical image are shown in figure 4.

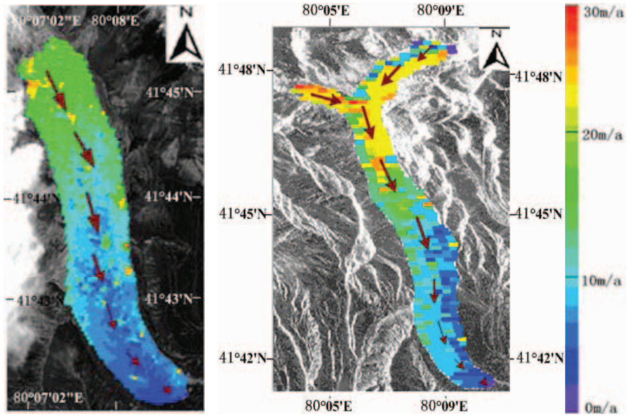

Figure 4. Flow field of the glacier from optical and SAR images. Optical images get flow field between 3600 m a.s.l to the terminus while SAR images get flow field between 4000 m a.s.l and the terminus of the Keqikaer glacier.

4. RESULTS ANALYSIS

Flow field calculated from optimal size window contains three characteristics: 1, it reflects glacier velocity clearly; 2, mismatched noises are reduced obviously than smaller sizes; 3, it keeps more velocity details than bigger sizes. In brief, flow field from best-size window contains maximum useful velocity information.

Flow fields obtained from both optical and SAR image show a trend that the glacier moves slower at the bottom and it moves faster as the elevation rises. The velocity maps confirm that this is a healthy and dynamic glacier. Despite some differences, the two respectively obtained velocity curves reveal high level of spatial consistency. It suggests that velocities obtained from two kinds of data can be validated against each other.

ACKNOWLEDGE

Our research is supported by Chinese Ministry of Science and Technology (2009CB723901) and Chinese Academy of Sciences (kzcx2-yw-301). Japan Aerospace Exploration Agency (JAXA) is gratefully acknowledged for contributing ALOS data to support our research.

5. REFERENCES

[1]IPCC(Intergovernmental Panel on Climate Change), Forth Assessment Report. Working Group I, Cambridge University Press, pp.356-359, 2007.

[2]T.E.Khromova, G.B.Osipova, D.G.Tsvetkov, M.B. Dyurgerov, R.G. Barry, "Changes in glacier extent in the eastern Pamir, Central Asia, determined from historical data and ASTER imagery", Remote sensing of environment, 102, pp.24-32, 2006.

[3]E Trouvé, G Vasile, M Gay, L Bombrun, P. Grussenmeyer, T. Landes, J. Nicolas, P. Bolon, I. Petillot, A. Julea, L. Valet, J.Chanussot, M. Koehl"Combining Airborne Photographs and Spaceborne SAR Data to Monitor Temperate Glaciers Potentials and Limits", IEEE Transactions on Geoscience and Remote Sensing, vol45,no4, pp905-924, 2007.

[4] E Berthier, H Vadon, D Baratoux, Y Arnaud, C. Vincent, K.L. Feigl, F. Rémy, B. Legrésy, "Surface motion of mountain glaciers derived from satellite optical imagery", Volume 95, Issue 1, pp.14-28,2005